

## ANALYSIS OF NANOWEAR AND THIN FILMS USING AES AND XPS

### ANALIZA NANOBRABE IN TANKIH PLASTI Z UPORABO AES IN XPS

**John T. Grant**

Research Institute, University of Dayton, 300 College Park, Dayton, Ohio, 45469-0168, USA  
j.grant@ieee.org

*Prejem rokopisa - received: 2002-10-11; sprejem za objavo - accepted for publication: 2002-12-16*

Auger electron spectroscopy (AES) and X-ray photoelectron spectroscopy (XPS) have been used to characterize the nanowear of ZnO, the interdiffusion of Al/Ti films grown on SiC, contamination formed during the fabrication of MEMS (Micro-Electro-Mechanical Systems) switches, and the surface composition along a crack in an aluminum alloy. The relatively high spatial resolution of AES is very useful for the surface compositional analysis of MEMS devices and can often provide additional information about surface chemistry. When spatial resolution is not a problem, XPS usually provides superior quantitative analysis as well as more chemical information about the surface composition.

Key words: Auger electron spectroscopy, X-ray photoelectron spectroscopy, MEMS, wear, diffusion, contamination

Spektroskopija Augerjevih elektronov (AES) in rentgenska fotoelektronska spektroskopija (XPS) sta bili uporabljeni za karakterizacijo nanoobrade ZnO, interdifuzije v Al/Ti plasteh na podlagi SiC, kontaminacije med izdelavo MEMS (mikromehanskih sistemov) in sestave površine vzdolž razpoke v aluminijevi zlitini. Relativno velika prostorska ločljivost AES je zelo uporabna za analizo površine MEMS-naprav in lahko prinese dodatne informacije o sestavi površine. Ko ni problem prostorska ločljivost, XPS prinaša boljše kvantitativne podatke in več podatkov o kemijski sestavi površine.

Ključne besede: spektroskopija Augerjevih elektronov, rentgenska fotoelektronska spektroskopija, MEMS, obraba, difuzija, kontaminacija površine

## 1 INTRODUCTION

Auger electron spectroscopy (AES) and X-ray photoelectron spectroscopy (XPS), (XPS is also called ESCA, electron spectroscopy for chemical analysis), are commonly used techniques for determining the surface composition of materials. In AES and XPS applications, there is often a need for high spatial resolution, for example in studying MEMS-related devices. The spatial resolutions of AES and XPS instruments have improved over the years, with modern commercial instruments being able to acquire spectra from areas of the order of 10 nm (AES) and 10  $\mu\text{m}$  (XPS). With AES, the regions to be analyzed are determined by operating the instrument in the SEM mode and measuring the secondary electrons or backscattered electrons leaving the sample, or by measuring changes in the current to ground, to form an image of the surface as the electron beam is rastered on the sample. With XPS, regions to be analyzed are located by (previously calibrated) optical microscopes, video cameras, X-ray induced electron emission, or by imaging the sample through the analyzer. Higher spatial resolutions with XPS can be achieved by conducting the analysis at a synchrotron, where spatial resolutions of the order of 100 nm can be achieved. This paper describes the application of AES to study the nanowear of ZnO, the interdiffusion of Al/Ti films grown on SiC, and to identify contamination formed

during the fabrication of MEMS switches. XPS was used to determine the surface composition along a crack in an aluminum aircraft alloy, and also to study the contamination formed during the fabrication of the MEMS switches.

## 2 EQUIPMENT

For the AES analysis, a Physical Electronics Inc (PHI) model 5700 AES/XPS system was used. For the XPS analysis, a Surface Science Instruments (SSI) M-Probe was used. The electron gun on this PHI system has a minimum electron beam diameter of 100 nm at 10 keV. Secondary electrons were used for imaging the sample surface. The highest spatial resolution of the SSI M-probe is 150  $\mu\text{m}$  in diameter, with the maximum analysis area being a rectangle 400  $\mu\text{m}$   $\times$  1000  $\mu\text{m}$ . In the SSI system, the analysis area is determined by the size of the monochromatic Al X-ray beam on the sample, and the sample is positioned in the analysis chamber using an optical microscope. Both of these systems have fast sample insertion capabilities, so analysis can be started within 1/2 hour after mounting the sample on a holder. The SSI system has a larger sample introduction port allowing samples of 25 mm height to be inserted, whereas this PHI system is limited to samples 15 mm high.

### 3 AES STUDY OF THE NANOWEAR OF ZnO

In ambient conditions, zinc oxide thin films can show low friction and long wear life, and this is thought to be due to extra defects introduced into the ZnO by preferred doping. This hypothesis was examined by J. Nainaparampil<sup>1</sup>, by studying the nanowear of ZnO crystal faces by prolonged scanning (tribological stressing) with the Si tip of an atomic force microscope (AFM). Continuous scanning with the Si tip would be expected to form transfer films at the nano-wear scar and produce a reduction in friction, as Si is one of the preferred dopants. The pyramidal tip of the AFM had a height of 3 μm, an apex angle of 15°, and a circular base with a radius of 1 μm. Lateral force measurements showed that the nanowear scar had a lower friction coefficient than the surrounding areas<sup>1</sup>, so AES was used to examine the wear scar for the presence of Si. A nanowear scar is shown in **Figure 1**.

Auger spectra were measured inside the nanowear scar, and outside on the surrounding area. The Auger spectra are shown in **Figure 2**. As the scarred area could not be seen in the AES system using SEM imaging, the area scarred by the AFM was referenced to the edge of a mesh (a cut TEM grid) so it could be located in the AES system. **Figure 2a** shows the three Zn transitions (40-110 eV) from ZnO in the un-worn surrounding region (lower spectrum). The upper spectrum in **Figure 2a** was taken from the nanowear scar and shows the additional presence of Si. The presence of Si in the nanowear scar was confirmed using the high energy Si KL<sub>2,3</sub>L<sub>2,3</sub> transition as shown by the upper spectrum in **Figure 2b**; the lower spectrum is from the surrounding un-worn area. The spectra shown here are in derivative form and were obtained from the raw, direct spectra using differentiation in the computer. Auger signals were detected from Zn, O, C, and Si in the nanowear scar, and their atomic concentrations were calculated from the peak-to-peak intensities of the derivative Auger spectra, giving atomic concentrations of 20, 13, 65, and 2%, respectively. The corresponding atomic concentrations

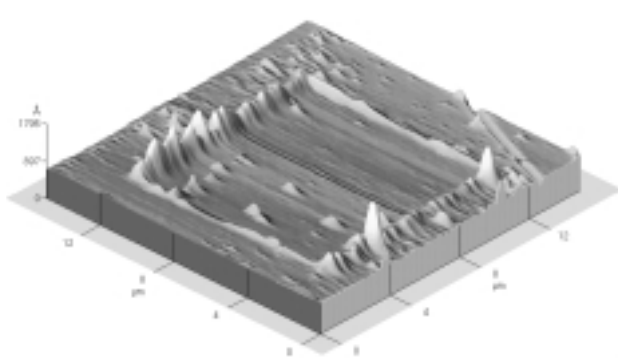


**Figure 1:** Nanowear scar on a ZnO crystal produced by prolonged scanning with the Si tip of an atomic force microscope (AFM)

**Slika 1:** Raza zaradi nanoobrade na kristalu ZnO, ki je nastala pri podaljšanem skeniranju s Si-konico v mikroskopu na atomsko silo

for Zn, O, and C from the un-worn surrounding area were 19, 11, and 70%, respectively. Si was not detected in the un-worn area. These calculations assume that the analyzed regions are homogeneous.

An energy dispersive spectroscopy (EDS) study of the worn tip showed the presence of Zn, which came from the ZnO crystal<sup>1</sup>.

In summary, prolonged scanning of a Si AFM tip on a ZnO (0001) surface resulted in a lubricious surface, and AES proved there was a transfer of Si from the tip to the ZnO.

### 4 THE INTERDIFFUSION OF Al/Ti FILMS GROWN ON SiC

A number of Al/Ti films grown on SiC were examined after being annealed at different temperatures. The goal was to determine if and when interdiffusion between the deposited layers occurred. AES was ideally suited for this study, as sputter depth profiles through the films will show when diffusion occurred. Linear least squares (LLS) fitting of the spectra also allowed Auger peak overlap problems to be removed, to determine if different chemical states of the elements exist in the layered structure, and to improve the signal-to-noise in

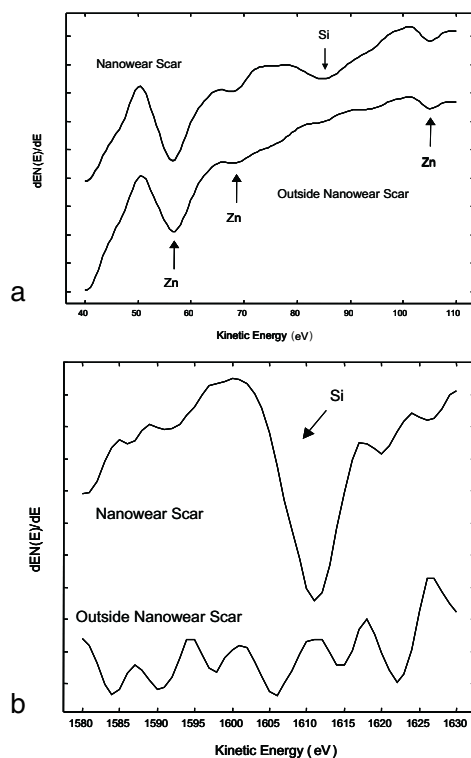


**Figure 2:** Auger spectra from inside the nanowear scar (upper spectrum), and outside on the surrounding area (lower spectrum); (a) low kinetic energy region (40 - 110 eV), and (b) high kinetic energy region (1580 - 1630 eV)

**Slika 2:** AES-spektri iz notranjosti raze (zgornji spekter) in iz njene zunanosti na površini v okolici (spodnji spekter); (a) nizka kinetična energija (40-110) eV in (b) področje z visoko kinetično energijo (1580-1630) eV

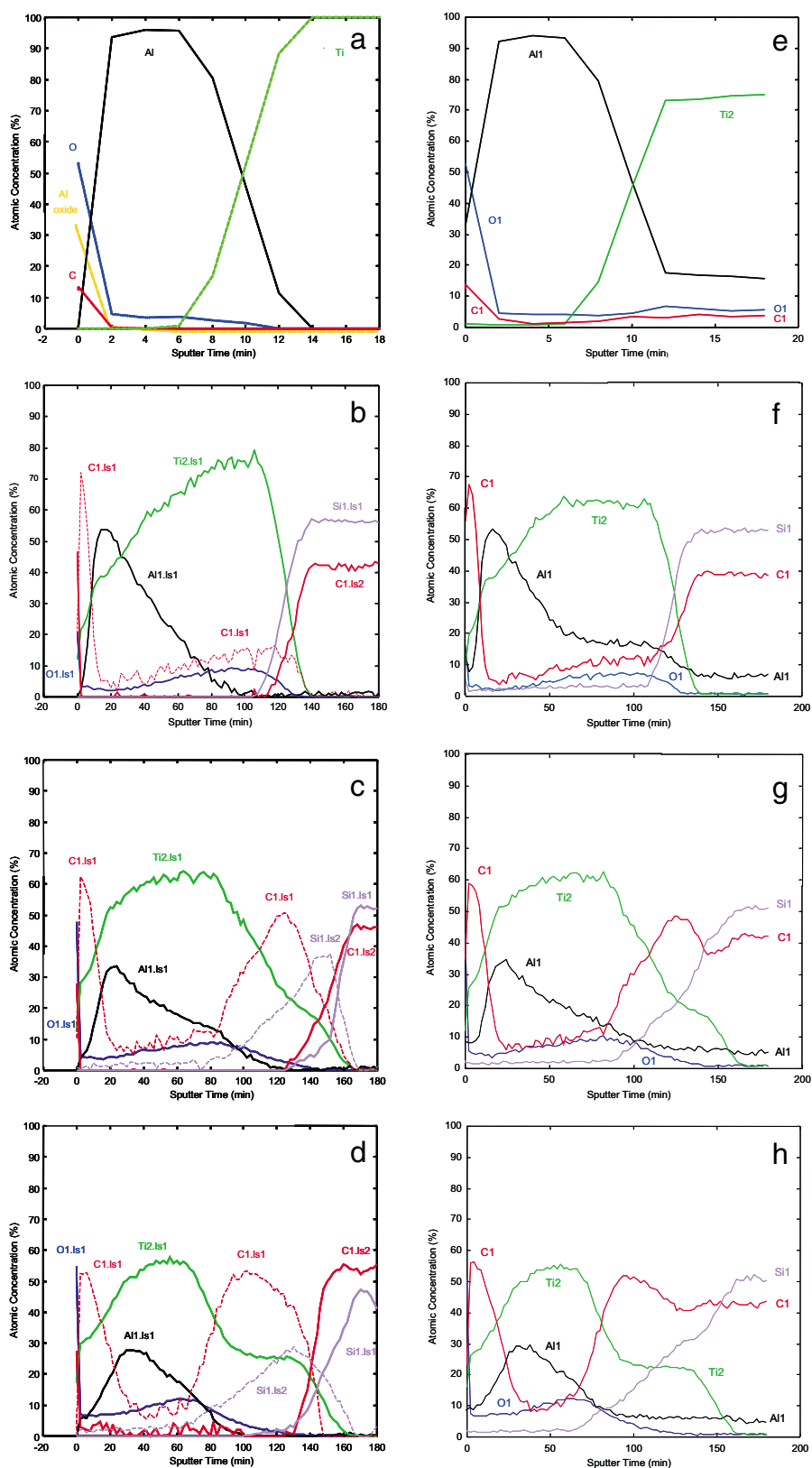


**Figure 3:** Sputter depth profiles of Al/Ti films on SiC using AES; a - d obtained using linear least squares (LLS) fitting of derivative spectra, (a) unannealed, (b) after annealing at 700 °C, (c) after annealing at 850 °C, and (d) after annealing at 1000 °C; e - h obtained directly from derivative spectra without LLS fitting, (e) unannealed, (f) after annealing at 700 °C, (g) after annealing at 850 °C, and (h) after annealing at 1000 °C

**Slika 3:** Profilni AES-diagram Al/Ti plasti na SiC; a-d pripravljene z uporabo najmanjših kvadratov (LLS) s prilagajanjem diferenciranih spektrov, (a) nežarjeno, (b) po žarjenju pri 700 °C, (c) po žarjenju pri 850 °C, in po žarjenju pri 1000 °C; e - h pripravljene neposredno iz diferenciranih spektrov brez LLS-obdelave, (e) nežarjeno, (f) po žarjenju pri 700 °C, (g) po žarjenju pri 850 °C in (h) po žarjenju pri 1000 °C

the profile <sup>2</sup>. Four sets of films were examined, one being unannealed, the others where samples had been annealed at 700, 850, and 1000 °C.

A 10 nA, 5 keV electron beam was used for the Auger measurements, and a 2 mm × 2 mm rastered, 3 keV Ar<sup>+</sup> ion beam was used for sputtering. Auger measurements and sputtering were alternated to prevent complications from ion excited Auger emission within the Al film; see below <sup>3</sup>.

The unannealed sample showed no significant interdiffusion between the Al and Ti layers, as can be seen from the profile in **Figure 3a**. A limited number of measurements were made in this profile. Note the presence of an aluminum oxide layer at the surface, and the presence of a few atomic percent O in the Al film.

On the other hand, all the annealed samples showed various degrees of interdiffusion as can be seen in the profiles in **Figures 3b-d**.

Significant interdiffusion can be seen after annealing at 700 °C, **Figure 3b**. Ti was detected at the surface before sputtering. As soon as the surface carbon contamination was removed (after one sputtering cycle), the C Auger lineshape changed (curve C1.ls1) and was typical for that from a metal carbide <sup>4</sup>. Therefore, it appears that titanium carbide is present during the first several minutes of sputtering. The C concentration then decreased significantly, but some titanium carbide was found throughout the remaining Ti-containing region. The Al concentration was very low near the surface, increased rapidly below the titanium carbide layer, and then decreased within the remaining Ti region. Oxygen was also detected throughout the Al-Ti region, and dropped to zero within the SiC. The SiC substrate was quite obvious, and the C lineshape here (curve C1.ls2) is different from that of a metal carbide and is typical for that from SiC <sup>4</sup>.

After annealing at 850°C, **Figure 3c**, significant reaction with the SiC substrate was also observed. The C lineshape is that of a metal carbide (curve C1.ls1) both near the surface and near the SiC substrate, indicating the presence of titanium carbide in these regions. Some titanium carbide is also present throughout the intermediate titanium layer. Oxygen is also present throughout the titanium region. Again, the aluminum concentration near the surface is low, and appears to have diffused further into the titanium region. There is also a different Si lineshape (curve Si1.ls2) near the SiC substrate, perhaps due to a titanium silicide.

The sputter depth profile measured after annealing at 1000 °C, **Figure 3d**, showed further reactions. The carbide layers (curve C1.ls1) appeared wider, with a corresponding change in the Ti distribution (curve Ti2.ls1). The apparent titanium silicide layer near the SiC substrate also seems to have grown wider. The Ti Auger transitions used in all these profiles were the LMM transitions near 420 eV. Similar profiles were

obtained using the LMM transitions near 390 eV. The Al and Si transitions used were the L<sub>2,3</sub>VV.

The sputter depth profiles shown in **Figures 3a-d** were obtained using LLS fitting in PHI-Multipak <sup>5</sup>. If quantitative analysis was carried out using the peak to peak heights in the derivative data without LLS fitting, the profiles shown in **Figures 3e-h** are obtained. Note that without Auger lineshape analysis to separate out different chemical components of the elements detected, interpretation of the sputter depth profiles in **Figures 3e-h** is not obvious. The signal to noise is also poorer, and it appears that elements are present in some regions where they are not present. For example, in comparing **Figures 3a and e** (unannealed films), the unprocessed data (**Figure 3e**) indicates the presence of aluminum within the titanium layer, even though it is not present (**Figure 3a**). This apparent aluminum signal is due to a sloping background in the aluminum energy window when in the titanium layer. Note that LLS processing removes the error in aluminum concentration due to this background (**Figure 3a**).

If the sputter depth profiles were obtained with the electron and ion beams on together (as is often done in AES), a sputter depth profile shown in **Figure 4** was obtained for the unannealed films. The ion beam energy was 3 keV. The profile, for the conditions used here, is now dominated by the ion-excited Al and Si peaks <sup>3</sup>, and using the electron-excited sensitivity factors for Al and Si (supplied by the manufacturer) gives quite an erroneous profile as the sensitivity factors used for Al and Si are now too small.

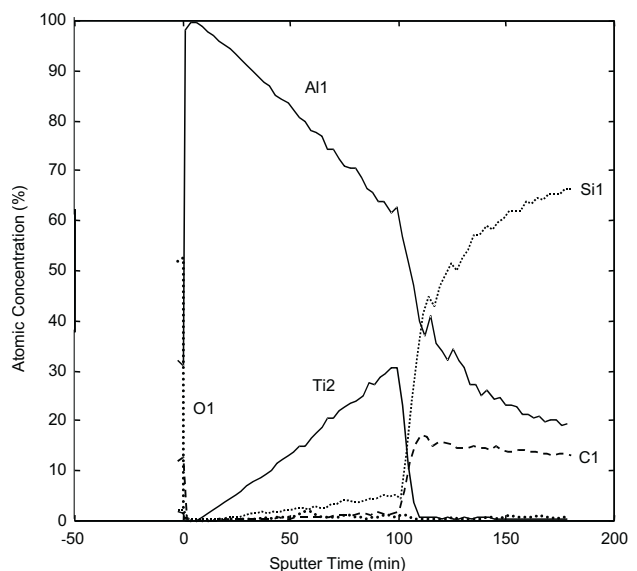


**Figure 4:** Sputter depth profile of unannealed Al/Ti on SiC using AES, with a 3 keV Ar<sup>+</sup> ion beam on during Auger data acquisition. The ion-excited signals from Al and Si dominate the profile and give an erroneous quantitative analysis

**Slika 4:** Profilni AES-diagram nežarjenega Al/Ti na SiC, določen z ionskim jedkanjem Ar<sup>+</sup>, 3 keV. Ionsko vzbujena signala Al in Si prevladujeta in dajeta nepravilno kvantitativno analizo.

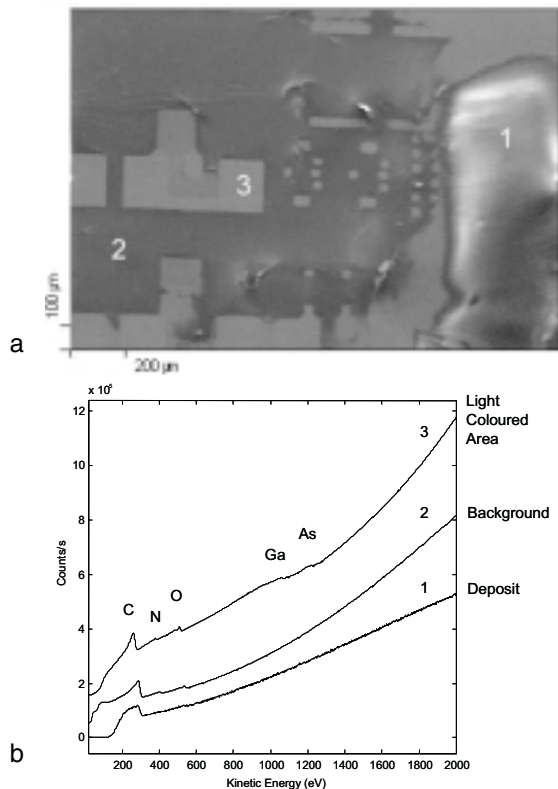


**Figure 5:** (a) SEM secondary electron image of part of a MEMS switch being fabricated on GaAs. The region marked 1 is contaminating residue left after stripping the photoresist; (b) Auger spectra obtained from the regions marked 1, 2, and 3 in part (a)

**Slika 5:** (a) SEM-slika dela MEMS-stikala, ki je bilo izdelano na GaAs. Področje, označeno z 1, je kontaminacijski ostanek po jedkanju z fotorezistom, (b) AES-spektri področij, označenih z 1, 2, 3 in deloma (a)

In summary, this analysis shows the usefulness of AES sputter depth profiling to monitor the interdiffusion of Al/Ti layers on SiC after annealing, and how the information in, and the quality of, the profiles were enhanced by linear least squares fitting of the data.

**5 CONTAMINATION DURING THE FABRICATION OF MEMS SWITCHES**

An unknown white residue was observed after stripping the photoresist in RF MEMS switch fabrication on GaAs substrates. Several pieces of residue could be seen, the largest being about 500 μm in size. When this sample was received, the PHI system (for AES analysis) was not available so some XPS work was performed with the limited spatial resolution of the SSI system.

The XPS analysis of the largest piece of white residue gave surface concentrations of 75 at. % C, 20 at. % O, with the remainder being N (this assumed that the surface composition was homogeneous in the analyzed region). A region away from the white residue gave similar relative concentrations of C, O and N, but with about 0.7 at. % each of Ga and As. This region was known to be inhomogeneous, due to the patterning made

on the device. This XPS analysis showed that the deposit was thick enough to prevent signal being detected from the GaAs substrate (as expected) and was probably due to photoresist. However, with the small size of the residue there was some uncertainty regarding the position of the 150 μm X-ray beam on the sample using the microscope for alignment, as this system is used by many people for various projects, and an alignment calibration of the microscope was not performed just prior to analysis. AES analysis in the PHI system was therefore planned for later.

The residue could be easily located using the electron beam in the PHI system. An SEM image from part of the sample is shown in **Figure 5a**, where the deposit appears as the large region (labeled 1) at the right. Note also the patterned areas on the sample. Auger spectra taken from the three areas marked in **Figure 5a** are shown in **Figure 5b**. Note that the patterned area (labeled 3) shows Ga and As signals from the substrate, whereas the other two areas do not. The C signal from region 1 is broader than that from regions 2 and 3 and indicates electrical charging in region 1.

This AES analysis showed that the residue was organic with a composition similar to photoresist. The white residue occurred due to the apparent interaction of photoresist and a low power RF bias plasma sputter cleaning process. The plasma cleaning altered the state of the photoresist in some areas such that standard photoresist stripping solutions did not remove the residue that formed. Based on this analysis, the photolithography processing steps were modified to eliminate this problem.

**6 THE SURFACE COMPOSITION ALONG A CRACK IN AN ALUMINUM AIRCRAFT ALLOY**

XPS was used to determine the composition at different places along a crack in an aluminum structural part from an aircraft. The crack was long, approximately 25 cm, so the part had been cut into five sections along its length, and then cut from behind so each part was about

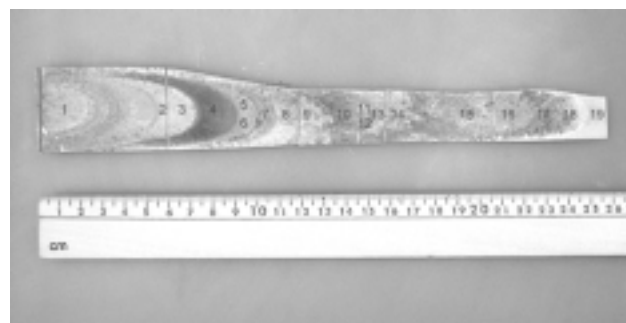


**Figure 6:** A photograph of a crack in an aluminum structural part from an aircraft. The 19 places marked show where XPS analysis was performed.

**Slika 6:** Posnetek razpoke na delu letala iz aluminija. Na 19 označenih mestih je bila izvršena XPS-analiza.

**Table 1:** Atomic concentrations of elements detected at the 19 regions examined along the crack shown in **Figure 6**. The concentrations are in atomic percent, and assume that the surface is homogeneous within each 400 μm x 1000 μm analysis area. Region 14 was analyzed twice, the second analysis being for a much longer time (improved signal to noise and detectability).

**Tabela 1:**atomska koncentracija elementov na 19 mestih vzdolž razpoke na **sliki 6**. Predpostavljena je homogena sestava površine na področju 400x1000 μm. Točka 14 je bila analizirana dvakrat, trajanje druge analize je bilo daljše (izboljšano je razmerje med signalom in ozadjem ter občutljivost)

Location	Zn	O	Ca	C	Al	Cd	N	Mg	Na	Si	S	F	P	Cu	Cl
1	1.1	25	1.1	71		0.7	1.0						0.4		
2	1.0	23	1.5	70	2	0.7	0.8						1.4		
3	0.9	23	1.5	68	2	0.5	0.3					3.0	1.1		
4	1.1	30	1.0	59	5	0.1	0.5					1.5	0.8	0.1	
5	1.4	28	1.9	61	2	0.8	0.1		0.4			3.2	1.7		
6	1.2	24	1.7	68		0.6	0.4					2.5	1.5		
7	1.2	32	2.2	54	4	0.6	0.9					3.5	2.3		
8	1.4	33	2.6	54	4	0.8	0.1					2.1	2.8		
9	1.4	32	1.8	57	4	0.7	0.3						2.7		
10	1.4	31		60	5	0.4	0.6						1.7		
11	0.5	43	1.2	39	15		0.7								
12	0.7	46	2.1	38	13	0.03	0.1	0.0							
13	1.0	48	1.3	36	12	0.09	0.3	1.4					0.4		
14	1.1	39	2.5	47	6	0.3	0.4	0.8		0.9			1.2		
14	1.1	39	2.6	47	7	0.3	0.4	1.3	0.2	0.9	0.3		1.1		
15	0.7	54		17	22			5.9							
16	0.6	43		37	11		0.7	3.8	1.8	1.5	0.6				
17	0.4	42		35	16		0.7	4.9	0.5						
18	0.2	34		49	10		1.3	3.2	0.9	1.5	0.2				
19		30		46	14		1.5	4.3		3.2					0.5

2 cm thick. Cutting was required to make samples small enough so they could be inserted into the SSI system using the fast insertion system. Each section was mounted and analyzed separately. A photograph of the crack is shown in **Figure 6**. Analysis was performed at 19 places along the crack, corresponding to parts with different optical appearances. The elements detected, and their concentrations, are listed in **Table 1**.

As can be seen from **Table 1**, Cd, P and Ca were generally detected from the top of the crack, left side in **Figure 6**, analysis location 1, down to the top of section number 4 (location 14). Mg was detected on the lower half of the crack, and Al increased (generally) down the crack. About 1 atomic percent Zn was detected almost everywhere on the crack surface (Mg and Zn are present in the aluminum alloy). Section number 2 showed a few atomic percent F at all locations (locations 3 through 8),

but as none was found on the other specimens, it was most likely contamination from handling.

This compositional information was given to the customer, and it was determined that the Cd detected was from a fastener at the crack initiation point.

## 7 SUMMARY

The usefulness of AES for studying nanowear of ZnO, the interdiffusion of Al/Ti films on SiC, and identifying contamination formed during the fabrication of MEMS switches has been shown. The application of XPS to determine the surface composition down a long crack in an aluminum aircraft alloy has been shown, and it was also used to examine contamination formed during the fabrication of MEMS switches. Linear least squares fitting of sputter depth profile data was used to improve the interpretation of the data.

## Acknowledgements

The author would like to thank his colleagues for providing these samples for analysis: Jose Nainaparampil for the nanowear of ZnO; Mike Capano for the Al/Ti films on SiC; Kevin Leedy for the MEMS switch fabrication on GaAs; and, Deb Peeler for the crack in the Al aircraft alloy. The support of the U.S. Air Force Research Laboratory in conducting these analyses is also gratefully acknowledged.

## 8 REFERENCES

- <sup>1</sup> J. J. Nainaparampil, J. T. Grant, and J. S. Zabinski, in submission
- <sup>2</sup> W. F. Stickle, and D. G. Watson, *J. Vac. Sci. Technol. A*, 10 (1992) 2806
- <sup>3</sup> J. T. Grant, M. P. Hooker, R. W. Springer, and T. W. Haas, *J. Vac. Sci. Technol.* 12 (1975) 481
- <sup>4</sup> T. W. Haas, J. T. Grant, and G. J. Dooley, *J. Appl. Phys.*, 43 (1972) 1853
- <sup>5</sup> PHI - Multipak, Physical Electronics, Inc., Eden Prairie, Minnesota, USA